
**Max Planck Institute Magdeburg**
**Preprints**

Martin Hess  Sara Grundel  Peter Benner

# Estimating the Inf-Sup Constant in Reduced Basis Methods for Time-Harmonic Maxwell's Equations


**MPIMD/14-19**  **November 4, 2014**

**Abstract**

The Reduced Basis Method (RBM) generates low-order models of parametrized partial differential equations (PDEs). These allow for the efficient evaluation of parametrized models in many-query and real-time contexts.

We use the RBM to generate low order models of micro scale semiconductor devices under variation of frequency, geometry and material parameters. In particular, we focus on the efficient estimation of the discrete stability constant, used in the Reduced Basis error estimation, which enables to generate low-order models with certified accuracy. A good estimation of this discrete stability constant is a challenging problem for Maxwell's equations. We therefore test and compare multiple techniques and discuss their properties in this context.

**Imprint:**

## Max Planck Institute for Dynamics of Complex Technical Systems, Magdeburg

**Publisher:**
Max Planck Institute for
Dynamics of Complex Technical Systems

**Address:**
Max Planck Institute for
Dynamics of Complex Technical Systems
Sandtorstr. 1
39106 Magdeburg

http://www.mpi-magdeburg.mpg.de/preprints/

# 1 Introduction

The Reduced Basis Method (RBM) generates low order models for the efficient solution of parametrized partial differential equations (PDEs) in real-time and many-query scenarios. One of its key features is that the RBM employs rigorous error estimators to perform the model reduction and to certify the accuracy of the reduced simulation. In recent years, the RBM has been developed to apply to a wide range of problems, of which [1] and the references therein, give an overview.

We address the use of the RBM for time-harmonic electromagnetic problems, which shows exponential convergence speed in the approximation error, see [2]. However, a computational bottleneck is in the construction of the error bound, namely the significant computational time required to estimate the inf-sup stability constant. Therefore, we replace the rigorous time-consuming successive constraint method by approximation methods. We give a detailed comparison of methods to estimate the stability constant to extend on previous work [2] and [3]. In particular, the so-called MinRes estimator, introduced in [4] shows superior performance compared to the other estimators.

Recent work in parametric model order reduction (PMOR) within the electromagnetic regime uses multipoint expansion techniques [5] and proper orthogonal decomposition (POD) [6]. Geometric parameter variations are also investigated in [5]. The RBM can also be extended to time-dependent Maxwell formulations, see [7] as an example.

Section 2 introduces the computational framework, while section 3 briefly covers the reduced basis model reduction and section 4 gives details on the error estimation. The main contribution of the paper is in section 5 and section 6. Section 5 derives different estimators for the discrete stability constant and in section 6 numerical comparisons are performed on the example of a coplanar waveguide. Section 7 concludes our findings.

# 2 Model Problem

We consider the second order time-harmonic formulation of Maxwell's equations in the electric field $E$

$$\nabla \times \mu^{-1} \nabla \times E + j\omega\sigma E - \omega^2 \epsilon E = j\omega J \quad \text{in } \Omega, \tag{1}$$

subject to essential boundary conditions $E \times n = 0$ on $\Gamma_{\text{PEC}}$ and Neumann boundary conditions $\nabla \times E \times n = 0$ on $\Gamma_{\text{PMC}}$, where $\partial\Omega = \Gamma_{\text{PEC}} \cup \Gamma_{\text{PMC}}$. The source current density is denoted by $J$, the imaginary number $j$, the frequency $\omega$ and the material coefficients are the permeability $\mu$, conductivity $\sigma$ and permittivity $\epsilon$.

The field solution is sought in the space $H(\text{curl})$ which is the set of functions

$$H(\text{curl}) = \{u \in (L^2(\Omega))^3 | \nabla \times u \in (L^2(\Omega))^3\}, \tag{2}$$

with corresponding norm

$$\|u\|_{H(\text{curl})} = (\|u\|^2_{(L^2(\Omega))^3} + \|\nabla \times u\|^2_{(L^2(\Omega))^3})^{\frac{1}{2}}. \tag{3}$$

The parameter vector $\nu$ is introduced to denote parametric dependence in frequency $\omega$, geometry (which is varied by varying $\Omega$ and or $\Gamma_{\mathrm{PEC}}$,$\Gamma_{\mathrm{PMC}}$) or material coefficients $(\mu, \sigma, \epsilon)$. The parameter dependent weak form with test function $w$ to (1) is established with sesquilinear form

$$a(E, w; \nu) = \left(\mu^{-1}\nabla \times E, \nabla \times w\right) + j\omega\left(\sigma E, w\right) - \omega^2\left(\epsilon E, w\right) \tag{4}$$

using the complex $L_2$-inner product $(\cdot, \cdot)$ over $\Omega$ and the linear form

$$f(w; \nu) = j\omega\left(J, w\right) \tag{5}$$

as

$$a(E(\nu), w; \nu) = f(w; \nu) \quad \forall w \in \mathcal{X}, \tag{6}$$

using the function space

$$\mathcal{X} = \{u \in H(\mathrm{curl}) | u \times n = 0 \text{ on } \Gamma_{\mathrm{PEC}}\}. \tag{7}$$

The Neumann boundary conditions on $\Gamma_{\mathrm{PMC}}$ are natural boundary conditions and are therefore implicit in the weak formulation of the problem.

After discretization with $H(\mathrm{curl})$-conforming Nédélec finite elements [8], solving (6) reduces to solving a sparse linear system

$$Ax = j\omega b, \tag{8}$$

for the state vector $x \in \mathbb{C}^{\mathcal{N}}$ of large dimension $\mathcal{N}$, which represents the electric field solution $E = \sum x_i \phi_i$ in the discrete space $X$, which is composed of basis functions $\{\phi_j | j = 1, ..., \mathcal{N}\}$, s.t.

$$X = \mathrm{span}\{\phi_j | j = 1, ..., \mathcal{N}\}. \tag{9}$$

The associated inner product matrix of the discrete function space is denoted $M$. It is defined element-wise by

$$M_{ij} = (\phi_i, \phi_j). \tag{10}$$

The $X$-norm of a vector $x$ is thus computed as

$$\|x\|_X = \sqrt{x^T M x}. \tag{11}$$

When we are interested in the transfer behavior over a certain frequency range (i.e. $\nu = \omega$), the matrix $A$ is affinely decomposed into parameter-independent matrices as

$$A = A^\mu + j\omega A^\sigma - \omega^2 A^\epsilon, \tag{12}$$

where the matrices $A^\mu$, $A^\sigma$ and $A^\epsilon$ are discretizations of the respective parts of the weak form, defined element-wise by

$$A^\mu_{ij} = \left(\mu^{-1}\nabla \times \phi_i, \nabla \times \phi_j\right), \tag{13}$$

$$A^\sigma_{ij} = (\sigma\phi_i, \phi_j) = \sigma M, \tag{14}$$

$$A^\epsilon_{ij} = (\epsilon\phi_i, \phi_j) = \epsilon M, \tag{15}$$

and right-hand-side vector $b$, defined as

$$b_i = (J, \phi_i). \tag{16}$$

PEC boundary conditions are incorporated by setting the appropriate degrees of freedom to zero and PMC boundary conditions are treated as natural boundaries.

Splitting the state vector $x$ into real and complex parts $x = x_{real} + jx_{imag}$ and using (12), the complex linear system can be rewritten as an equivalent system of twice the dimension over the real numbers

$$\begin{bmatrix} A^\mu - \omega^2 A^\epsilon & -\omega A^\sigma \\ -\omega A^\sigma & -A^\mu + \omega^2 A^\epsilon \end{bmatrix} \begin{bmatrix} x_{real} \\ x_{imag} \end{bmatrix} = \begin{bmatrix} 0 \\ -\omega b \end{bmatrix}. \tag{17}$$

This leads to a real and symmetric system matrix, thus its spectrum is real, which is advantageous for the computation of eigenvalues required in the error estimation process.

In the case of multiple parameters a similar affine decomposition can be readily established, see [1] or [3] for the treatment of geometric parameters:

$$A^\nu = \sum_{q=1}^{Q_a} \Theta_a^q(\nu) A^q.$$

In the following, we will denote by $E(\nu)$ either the parameter-dependent $2\mathcal{N}$-dimensional solution vector to the real system (17) or the corresponding function in $X$. In that context we can rewrite the bilinear form $a(\cdot, \cdot; \nu)$ defined over the $H(\mathrm{curl})$ conforming finite element space $X$ by the system matrix $A^\nu$ from (17) as

$$\begin{aligned} a(E(\nu), w; \nu) &= E(\nu)^T A^\nu w \\ &= E(\nu)^T \begin{bmatrix} A^\mu - \omega^2 A^\epsilon & -\omega A^\sigma \\ -\omega A^\sigma & -A^\mu + \omega^2 A^\epsilon \end{bmatrix} w. \end{aligned} \tag{18}$$

The vector $w$ also has to be interpreted as an element in $R^{2\mathcal{N}}$ or an element of $X$ depending on the situation.

# 3 Reduced Basis Method for time-harmonic EM-problems

The aim of the RBM is to determine a low order space $X_N \subset X$ of dimension $N$, which approximates the parametric solution manifold $M^\nu = \{E(\nu) \in X | \nu \in \mathcal{D}\}$ well. Given such a space $X_N$, it is possible to gain accurate approximations $E_N(\nu) \in X_N$ to $E(\nu)$ by projecting (6) onto $X_N$, i.e. solve

$$a(E_N(\nu), w_N; \nu) = f(w_N; \nu) \quad \forall w_N \in X_N.$$

Due to the affine decomposition (as seen in Section 2 and more detailed in [1, 2, 3]) of the bilinear and linear form, they can be written as

$$a(E(\nu), w; \nu) = \sum_{q=1}^{Q_a} \Theta_a^q(\nu) a^q(E(\nu), w), \tag{19}$$
$$f(w; \nu) = \sum_{q=1}^{Q_f} \Theta_f^q(\nu) f^q(w).$$

Here $Q_a$ and $Q_f$ are reasonably small. Using the affine decomposition allows evaluating the error estimator with an algorithmic complexity that is independent of the full order discretization size [1].

An integral part in the model reduction are error estimators $\Delta_N(\nu)$, which give rigorous bounds to the approximation error in the discrete $H(\text{curl})$ norm.

$$\|E(\nu) - E_N(\nu)\|_X \leq \Delta_N(\nu). \tag{20}$$

The error estimation is at the heart of this paper and we will concentrate on its computation.

# 4 Error Estimation

The error estimation is developed using the dual space $X'$ of $X$. The dual space $X'$ is defined as the space of linear functionals $\phi : X \to \mathbb{R}$. The dual norm is defined as

$$\|\phi\|_{X'} = \sup_{v \in X} \frac{|\phi(v)|}{\|v\|_X}. \tag{21}$$

According to the Riesz representation theorem (as $X$ is a Hilbert space), the spaces $X$ and $X'$ are isometrically isomorph, i.e. for each $\phi \in X'$ there exists a unique $v \in X$ such that $\phi(\cdot) = (v, \cdot)_X$ and $\|\phi\|_{X'} = \|v\|_X$. In particular, it holds that $f(\cdot; \nu) \in X'$ and $a(u, \cdot; \nu) \in X'$.

Considering the residual $r(w, \nu) = a(E(\nu) - E_N(\nu), w, \nu)$ , we see that

$$\frac{\|r(\cdot, \nu)\|_{X'}}{\|E(\nu) - E_N(\nu)\|_X} \geq \inf_{u \in X} \frac{\|a(u, \cdot, \nu)\|_{X'}}{\|u\|_X} =: \beta(\nu),$$

with $\|r(\cdot; \nu)\|_{X'}$ the dual norm of the residual with respect to the full scale discretized problem. The constant $\beta(\nu)$ is called the discrete inf-sup stability constant, as it can be written as

$$\beta(\nu) = \inf_{w \in X} \sup_{v \in X} \frac{a(w, v; \nu)}{\|w\|_X \|v\|_X} \tag{22}$$

and if a lower bound $\beta_{LB}(\nu)$ is known, we have that the error between FEM and RB solutions is bounded by the error estimator

$$\|E(\nu) - E_N(\nu)\|_X \leq \Delta_N(\nu) = \frac{\|r(\cdot;\nu)\|_{X'}}{\beta_{LB}(\nu)}.$$

The computation of a rigorous lower bound to the discrete stability constant $\beta_{LB}(\nu)$ is the most time-consuming part in rigorous error estimation, especially when applied to Maxwell's equations, see [9]. As the computational effort for upper bounds is much less, we extend our investigations to methods actually computing upper bounds and compare their performance in approximating the parametrized discrete stability constant.

# 5 Discrete Stability Constant

The RBM typically employs a successive constraint method (SCM) to obtain lower bounds to the discrete stability constant. In particular the application to Maxwell's equations shows slow convergence, see [9].

As the computational complexity of the SCM for obtaining rigorous error estimators is often too high in the case of Maxwell's equations, we consider approximations $\beta_N(\nu) \approx \beta(\nu)$. In particular, we use the upper bounds derived from [9], and the MinRes and Galerkin estimators (method 1 and method 3 from [4]) and Kriging interpolation [10]. As $\beta_N(\nu)$ only approximates the discrete stability constant and is not a lower bound, these error estimators can be applied as in

$$\Delta_N(\nu) = \frac{\|r(\cdot;\nu)\|_{X'}}{\rho\beta_N(\nu)},$$

with $0 < \rho < 1$. However, numerical results indicate that the upper bounds of the MinRes estimator are tight and allow for a choice of $\rho$ close to one.

Introducing the Riesz representer, or supremizing operator $T^\nu$ defined via the relation $(T^\nu w, v)_X = a(w, v; \nu), \quad \forall v \in X$, it holds

$$\beta(\nu) = \inf_{w\in X} \frac{\|T^\nu w\|_X}{\|w\|_X},$$
$$\beta^2(\nu) = \inf_{w\in X} \frac{(T^\nu w, T^\nu w)_X}{(w, w)_X}.$$

The Riesz representer $T^\nu w$ satisfies the relation $T^\nu w = \arg\sup_{w\in X} \frac{a(w,\cdot;\nu)}{\|w\|_X}$ and is computed by solving a linear system with the inner product matrix ($MT^\nu = A^\nu$). One can compute the discrete stability constant by finding the eigenvector corresponding to the smallest eigenvalue of the matrix $A^\nu$, i.e. solve the generalized eigenvalue problem

$$A^\nu x = \lambda_{\min} M x \tag{23}$$

for the eigenvalue $\lambda_{\min}$ of minimum magnitude, which is equivalent to finding the smallest eigenvalue of $T^\nu$.

This is a large-scale, thus expensive eigenvalue problem, especially if one has to do it for multiple values of the parameter $\nu$.

While the eigenproblems considered here can be solved in MATLAB® using the *eigs* command, we also tried larger system sizes using the eigensolvers provided in the SLEPC framework. Here, the Jacobi-Davidson algorithm gave best results in accuracy and computation time for $\lambda_{\min}$. However, the total time required for obtaining rigorous error estimation was still significant even when using SLEPC [11, 12, 13].

## 5.1 SCM upper bounds

The affine decomposition (19) holds also for the operator $T^\nu$, in that $T^\nu w = \sum_{q=1}^{Q_a} \Theta_a^q(\nu) T^q w$, where the parameter-independent parts are defined via $(T^q w, v)_X = a^q(w, v), \quad \forall v \in X$. This allows to expand the stability constant as

$$(\beta(\nu))^2 = \min_{w \in X} \sum_{q'=1}^{Q} \sum_{q''=q'}^{Q} (2 - \delta_{q'q''}) \Theta^{q'}(\nu) \Theta^{q''}(\nu) \frac{\left(T^{q'} w, T^{q''} w\right)_X}{\|w\|_X^2}$$

with $\delta_{q'q''}$ the Kronecker delta.

Using $Z_{q'}^{q''}(\nu) = \Theta^{q'}(\nu)\Theta^{q''}(\nu)$ and symmetrization using elementary properties of the inner product $(\cdot,\cdot)_X$, it follows

$$\begin{aligned}(\beta(\nu))^2 = &\min_{w \in X} \sum_{q=1}^{Q} \left( Z_q^q(\nu) - \sum_{q'=1, q' \neq q}^{Q} Z_q^{q'}(\nu) \right) \frac{(T^q w, T^q w)_X}{\|w\|_X^2} \\ &+ \sum_{q'=1}^{Q} \sum_{q''=q'+1}^{Q} Z_{q'}^{q''}(\nu) \frac{\left(T^{q'} w + T^{q''} w, T^{q'} w + T^{q''} w\right)_X}{\|w\|_X^2}.\end{aligned}$$

Define

$$\begin{aligned} y_{q,q}(w) &:= \frac{(T^q w, T^q w)_X}{\|w\|_X^2}, \\ y_{q',q''}(w) &:= \frac{\left(T^{q'} w + T^{q''} w, T^{q'} w + T^{q''} w\right)_X}{\|w\|_X^2}, \end{aligned}$$

and the set $\mathcal{Y}$ as

$$\begin{aligned}\mathcal{Y} = \{ y = (y_{1,1}, ..., y_{Q,Q}) \in \mathbb{R}^{\frac{Q(Q+1)}{2}} \mid \\ \exists w \in X \text{ s.t. } y_{q,q} = y_{q,q}(w), y_{q',q''} = y_{q',q''}(w) \}.\end{aligned}$$

It thus holds $(\beta(\nu))^2 = \min_{y\in\mathcal{Y}} \mathcal{J}(\nu; y)$ with the objective function $\mathcal{J} : \mathcal{D}\times\mathbb{R}^{\frac{Q(Q+1)}{2}} \to \mathbb{R}$

$$\begin{aligned}\mathcal{J}(\nu; y) = &\sum_{q=1}^{Q}\left(Z_q^q(\nu) - \sum_{q'=1,q'\neq q}^{Q} Z_q^{q'}(\nu)\right) y_{q,q} \\ &+ \sum_{q'=1}^{Q}\sum_{q''=q'+1}^{Q} Z_{q'}^{q''}(\nu) y_{q',q''}.\end{aligned}$$

Let $C_K$ denote a set of $k$ parameter samples and define

$$Y_{UB}(C_K) = \{y^*(\nu_k)|y^*(\nu_k) = \arg\min_{y\in\mathcal{Y}} \mathcal{J}(\nu_k; y), \nu_k \in C_K\},$$

which is a subset of $\mathcal{Y}$.

Then derive the estimator for the squared stability constant as $\left(\beta_N^{SCM}(\nu)\right)^2 := \min_{y\in\mathcal{Y}_{UB}} \mathcal{J}(\nu, y)$, which satisfies $\beta_N^{SCM}(\nu) \geq \beta(\nu)$.

The set $C_K$ is obtained using typical sampling techniques. Here, we used Latin hypercubes (see [14]) as sample sets, but numerical examples indicate that a uniform deterministic sampling of the parameter domain yields about the same approximation quality as Latin hypercubes.

## 5.2 MinRes Estimator

An upper bound estimator can be derived by restricting the minimizing space to a subset $X_N \subset X$ and define

$$\beta(\nu) = \min_{w\in X} \frac{\|T^\nu w\|_X}{\|w\|_X} \leq \min_{w\in X_N} \frac{\|T^\nu w\|_X}{\|w\|_X} := \beta_N^{minres}(\nu).$$

Choose $X_N^{minres} = \{x(\nu_i)|i = 1\dots N\}\cup\{E(\nu_i)|i = 1\dots N\}$ as proposed in [4], where $x(\nu_i)$ is the eigenvector corresponding to $\beta(\nu_i)$. Then solve the generalized eigenvalue problem

$$X_N^T(A^\nu)^T M^{-1} A^\nu X_N x = \lambda_{\min} X_N^T M X_N x, \tag{24}$$

for the eigenvalue of minimum magnitude. Here, $X_N$ is a rectangular matrix of an orthonormalized basis of the space $X_N^{minres}$, i.e. we identify the matrix $X_N$ of full column rank with the linear subspace of $X$ which is spanned by the columns of $X_N$.

Taking the squared stability constant shows

$$\begin{aligned}\left(\beta_N^{minres}(\nu)\right)^2 &= \min_{w\in X_N} \frac{(T^\nu w, T^\nu w)_X}{(w,w)_X} \\ &= \min_{w\in X_N} \frac{w^T (T^\nu)^T M T^\nu w}{w^T M w} \\ &= \min_{w\in X_N} \frac{w^T (A^\nu)^T M^{-1} A^\nu w}{w^T M w},\end{aligned}$$

using $T^\nu = M^{-1}A^\nu$. The solution of (24) solves the minimization problem.

## 5.3 Galerkin Estimator

The Galerkin estimator is obtained when restricting the minimizing as well as maximizing space

$$\beta_N^{Galerkin}(\nu) = \min_{w\in X_N} \max_{v\in X_N} \frac{a(w,v;\nu)}{\|w\|_X \|v\|_X},$$

and is not necessarily an upper bound to the stability constant.

As the trial as well as test space is restricted, the large-scale eigenvalue problem (23) is projected onto $X_N$, i.e. solve for each parameter

$$X_N^T A^\nu X_N x = \lambda_{\min} X_N^T M X_N x \tag{25}$$

for the eigenvalue of minimum magnitude, which then serves as an estimate to the stability constant.

Alternatively, an estimator can be derived by solving

$$X_N^T M^{-1} A^\nu X_N x = \lambda_{\min} x \tag{26}$$

for the eigenvalue of minimum magnitude. We will briefly discuss using this approximation in the section on numerical results.

## 5.4 Kriging Interpolation Method

As a technique for interpolating functions depending on several parameters, Kriging is often used. It dates back to Krige's work of the 1950's. Even though it was originally used to approximate functions that have a non-deterministic character, it has become popular in computational science and engineering applications to create meta-models of black box functions that are expensive to evaluate. It gives in general better results than polynomial approximation. We will describe the basic idea and refer to [10] for a more detailed analysis.

Assume we have given $\nu_1, \ldots, \nu_n \in \mathbb{R}$ and the observation vector $B = [\ldots, \beta(\nu_i), \ldots]^T$. We are interested in creating an interpolant (meta-model) $\hat{\beta}$. In this setup, we assume that $\beta$ as well as its estimator $\hat{\beta}$ are random fields and that $\hat{\beta}$ is a linear combination of the given observations:

$$\hat{\beta}(\nu) = \sum_{i=1}^{n} \lambda_i(\nu)\beta(\nu_i) \tag{27}$$

such that the variance $\mathrm{Var}[\hat{\beta} - \beta]$ is minimized under the constraint that the expected value $E[\hat{\beta} - \beta] = 0$. We furthermore assume the random variable $\beta$ has a constant expected value and that the covariance function for $\beta$ is known.

$$E[\beta(\nu)\beta(\mu)] = R(\theta, \nu, \mu).$$

In our case the covariance function is given by a cubic spline and $\theta$ is determined during the algorithm to best approximate. For this we use the MATLAB® package DACE [15]. Another choice is the SUMO toolbox [16], where we would expect comparable results. Solving the minimization problem

$$\min_{\lambda} \mathrm{Var}[\hat{\beta} - \beta] \text{ s.t. } E[\hat{\beta} - \beta] = 0$$

under the assumptions discussed leads to the predictor

$$\hat{\beta}(\nu) = \sum_{i=1}^{n} \gamma_i R(\theta, \nu_i, \nu) + \delta, \tag{28}$$

where $\gamma$ and $\delta$ are the solutions to the linear problem:

$$\begin{pmatrix} R & e \\ e^T & 0 \end{pmatrix} \begin{pmatrix} \gamma \\ \delta \end{pmatrix} = \begin{pmatrix} B \\ 0 \end{pmatrix}.$$

R is a matrix with entries $R_{ij} = R(\theta, \nu_i, \nu_j)$ and $e$ is an $n$-dimensional vectors with entries of 1 everywhere. The linear system is solved using a direct solver, as the system is low-dimensional (the number of observations in our case is maximal 120). The estimator $\hat{\beta}$ is a realization to the given observation $B$.

To understand (28), we compute the Lagrange function:

$$\begin{aligned}
\mathcal{L}(\lambda, \mu) =& \mathrm{Var}[\hat{\beta} - \beta] + \mu E[\hat{\beta} - \beta] \\
=& E[(\hat{\beta} - \beta)^2] + \mu E[\hat{\beta} - \beta] \\
=& E[\hat{\beta}^2] - 2E[\hat{\beta}\beta] + E[\beta^2] + \mu E[\hat{\beta} - \beta] \\
=& E[\sum_{i=1}^{n}\sum_{j=1}^{n} \lambda_i\lambda_j\beta(\nu_i)\beta(\nu_j)] - 2E[\sum_{i=1}^{n} \lambda_i\beta(\nu_i)\beta] \\
&+ E[\beta^2] + \mu(\sum_{i=1}^{n} \lambda_i E[\beta(\nu_i)] - E[\beta(\nu)]) \\
&= \lambda^T R\lambda - 2r^T\lambda + E[\beta^2] + \mu(\lambda^T e - 1)E[\beta],
\end{aligned}$$

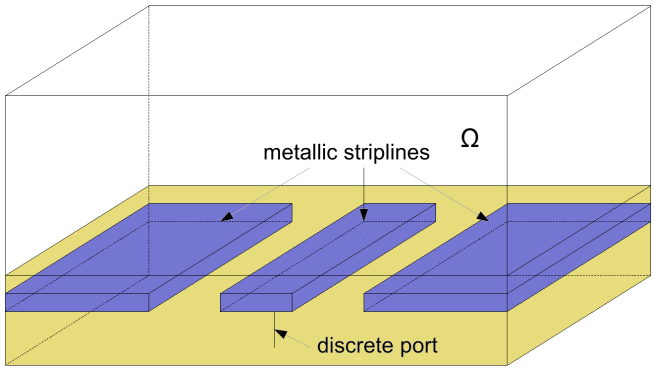


Figure 1: Geometry of coplanar waveguide. The forcing term $J$ is defined over the discrete port.

with $r_i(\nu) = R(\theta, \nu_i, \nu)$. Redefining $\mu$ as $1/2\mu E[\beta]$ and minimizing leads to

$$\begin{pmatrix} R & e \\ e^T & 0 \end{pmatrix} \begin{pmatrix} \lambda(\nu) \\ \mu(\nu) \end{pmatrix} - \begin{pmatrix} r(\nu) \\ 1 \end{pmatrix} = 0,$$

where $r_i(\nu) = R(\theta, \nu_i, \nu)$ and to a predictor $\hat{\beta}(\nu) = \lambda(\nu)^T B$ according to (27). This leads to

$$\begin{aligned} \hat{\beta} =& \lambda(\nu)^T B = \begin{pmatrix} \lambda(\nu)^T & \mu(\nu) \end{pmatrix} \begin{pmatrix} B \\ 0 \end{pmatrix} \\ =& \begin{pmatrix} \lambda(\nu)^T & \mu(\nu) \end{pmatrix} \begin{pmatrix} R & e \\ e^T & 0 \end{pmatrix} \begin{pmatrix} \gamma \\ \delta \end{pmatrix} \\ =& \begin{pmatrix} r^T & 1 \end{pmatrix} \begin{pmatrix} \gamma \\ \delta \end{pmatrix} = r^T \gamma + \delta = \sum_{i=1}^{n} \gamma_i R(\theta, \nu_i, \nu) + \delta. \end{aligned}$$

This means that our predictor is a radial basis function interpolation with radial basis function given by $R$ with linear detrending.

## 6 Numerical Results of Stability Constant Estimation

As an example model, we consider a coplanar waveguide[1], shown in Fig. 1. The model setup is contained in a shielded box $\Omega$ with perfect electric conducting (PEC) boundary on the ground. We consider three perfectly conducting strip lines as shown

[1] This model can be found in the Model Reduction Wiki, see morwiki.mpi-magdeburg.mpg.de.

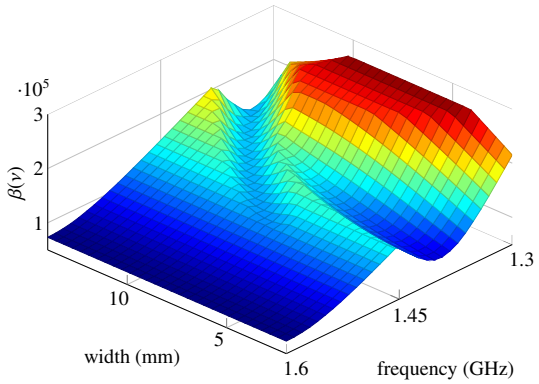


Figure 2: Stability constant plotted over variation of frequency and geometry.

in the geometry. The system is excited at a discrete port and the output is taken at a discrete port on the opposite end of the middle strip line. These discrete ports are used to model input and output currents/voltages.

The metal parts, i.e. the ground plate and the boundaries of the three metal sheets constitute $\Gamma_{\text{PEC}}$, where perfect electric conductance (PEC) is assumed.

The material coefficients are the permeability $\mu$, the conductivity $\sigma$ and the permittivity $\epsilon$. The metallic strip lines are immersed in a substrate of conductivity $\sigma = 0.02$ S/m and relative permittivity $\epsilon_r = 4.4$, shown colored in yellow in Fig. 1. In the upper part, the conductivity is $\sigma = 0.01$ S/m and relative permittivity $\epsilon_r = 1.07$. The relative permeability is $\mu_r = 1$ in the entire domain.

As parametric variation we look at the frequency $\omega \in [1.3, 1.6]$ GHz and the width of the middle strip line $p \in [2.0, 14.0]$ mm. In the three parameter model, we additionally consider that the conductivity in the lower part varies in $[0.005, 0.02]$ S/m and the conductivity in the upper part varies in $[0.01, 0.04]$ S/m. This variation is applied as a single parameter and it does not have a particular application in mind, but is used formally to investigate the estimators on a three parameter model.

The full simulation has been performed with the finite element package FEniCS. For our numerical experiments, we used a discretization size of $52'134$ degrees of freedom leading to the linear systems $A^\nu x = b^\nu$ of the discretization size. What RBM does is creating a small, still parameter dependent linear system that can be solved very fast.

We investigate the performance of different techniques for obtaining estimators to the discrete stability constant, such as successive constraint method upper bounds [9], the MinRes and Galerkin approximations derived in [4] and the Kriging interpolation method [10]. For the coplanar waveguide example, the discrete stability constant $\beta(\nu)$ is shown in Fig. 2 under parametric variation of frequency and the width of the middle strip line. Fig. 3 shows the three parameter example with additional parametric variation of the conductivity.

The two- and three-dimensional parametric domains are sampled using Latin hy-

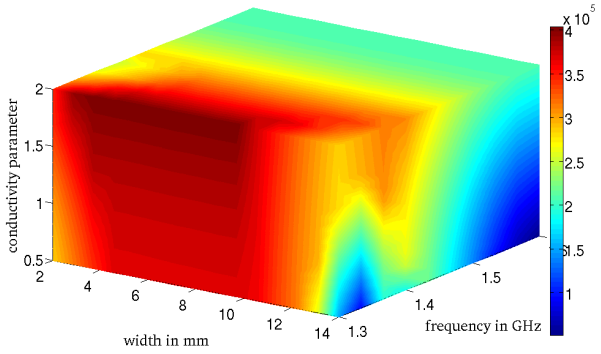


Figure 3: Stability constant plotted over variation of frequency, geometry and conductivity.

percubes and the eigenproblem corresponding to the computation of $\beta(\nu)$ is solved at these parameter locations. We plot the number of eigenproblems solved versus the relative approximation error to compare the approximation quality of the estimators, which gives a rough estimate of the main computational effort.

The numerical results of the mean error (Fig. 4 and Fig. 6) and the maximum error (Fig. 5 and Fig. 7) over a fine grid of the parameter domain show a clear indication for the MinRes estimator. It is the only estimator which resolves the stability constant with a mean error of less than 1%. The SCM upper bounds and the Kriging method also show convergence, but at a lower rate than the MinRes approximation, while the Galerkin estimator does not show convergence and probably requires a significantly larger train set.

The mean and maximum errors are computed by taking the mean/maximum over the relative errors $e_{rel}(\nu) = \frac{|\beta(\nu)-\beta_N(\nu)|}{\beta(\nu)}$ of a sampled grid of dimension $30 \times 35$ in the two parameter scenario and $10 \times 10 \times 15$ in the three parameter case. This grid is independent from the Latin hypercube samples used in the training process.

Table 1 shows the computation times of the estimators using five precomputed basis vectors (i.e. function evaluations in case of Kriging). The precomputation of the basis vectors took 160s, so this requires the largest portion of computational time. Thus, the computation of the estimators is dominated by evaluating the large-scale discrete stability constant, which is about 1.5 hours to generate the convergence plots.

Evaluating the Galerkin and Kriging estimators over the sample set has a negligible computational time. Also the SCM upper bounds (30s) and MinRes (12s) have a computational time which is much less than the function evaluations. The SCM bounds take a larger computation time as the evaluation of the objective functional $\mathcal{J}(\nu, y)$ for all $y \in \mathcal{Y}_{UB}$ is expensive. Taking into account the time required for function evaluations however, the computation times of the estimators are comparable for the model under consideration. In our test case a single function evaluation takes 32s, so

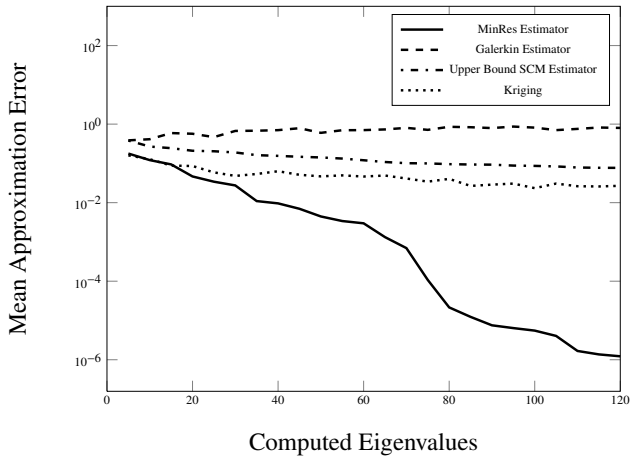


Figure 4: Convergence of mean error over fine reference sample set in the two parameter example. Plotted is the number of eigenproblems solved versus the mean relative approximation error.

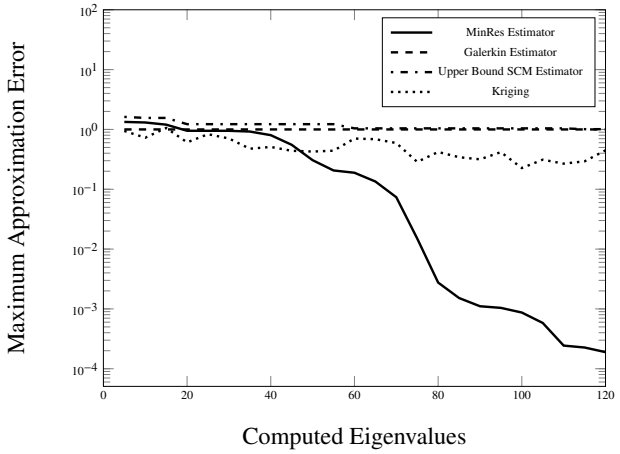


Figure 5: Convergence of maximum error over fine reference sample set in the two parameter example. Plotted is the number of eigenproblems solved versus the maximum relative approximation error.

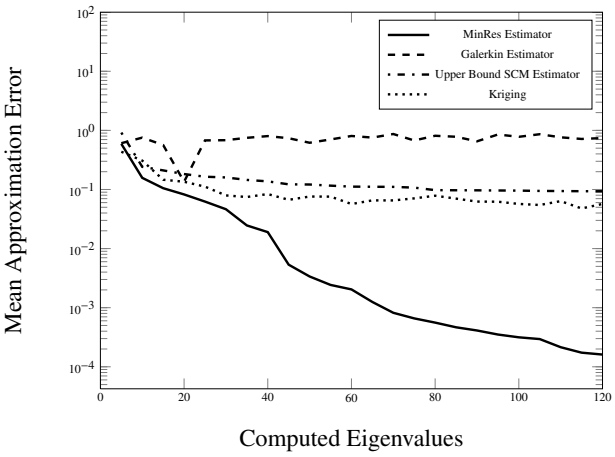


Figure 6: Convergence of mean error over fine reference sample set in the three parameter example. Plotted is the number of eigenproblems solved versus the mean relative approximation error.

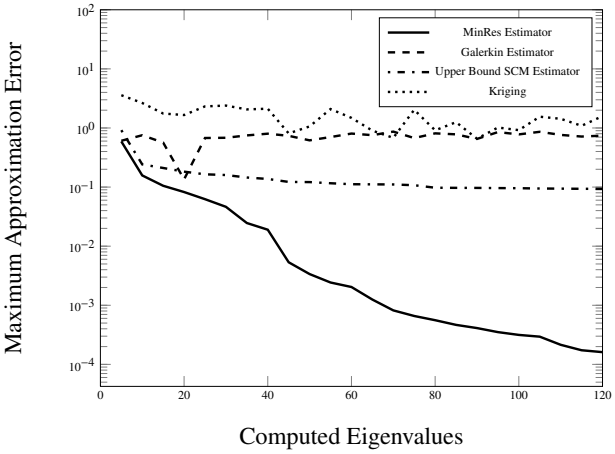


Figure 7: Convergence of maximum error over fine reference sample set in the three parameter example. Plotted is the number of eigenproblems solved versus the maximum relative approximation error.

Table 1: Comparison of Timings

| Estimator | Computation Time |
|---|---|
| **MinRes** | 12s |
| **Galerkin** | 0.6s |
| **SCM upper bounds** | 30s |
| **Kriging** | 0.6s |

Table 2: Improving MinRes

| Number of Eigenvectors | mean relative error |
|---|---|
| **1** | 0.1928 |
| **3** | 0.0152 |
| **5** | 0.0100 |

that adding additional observations in the Kriging for instance does exceed the total computation times of the other estimators.

In Table 2, the effect of using eigenvectors corresponding to the three and five smallest eigenvalues is investigated. The aim is to further increase the quality of the MinRes estimator. It uses 15 sample points in the two parameter example and collects the eigenvectors in the projection space $X_N$. The rationale behind this investigation is that the additional eigenvectors might serve as good approximations to the minimizers at other sample points. The numerical results show a significant improvement of the approximation quality for small increases in the number of eigenvalues. Also note that the computational time does not increase significantly by gathering additional eigenvectors.

The two variants of the Galerkin estimator (25) and (26) are compared in Table 3. Both tend to underestimate the stability constant, which leads to worse approximations when increasing the basis size. They are not effective for the model problem under consideration.

Table 3: Comparison of Galerkin variants

| No. of Eigenvectors | mean error (25) | mean error (26) |
|---|---|---|
| **120** | 0.800 | 0.352 |
| **240** | 0.693 | 0.440 |
| **360** | 0.812 | 0.466 |

# 7 Conclusion

The MinRes estimator clearly manages to resolve the stability constant better than all the other estimators. To use this estimator in a practical setting, a heuristic stopping criterion can be used, in the sense that if newly computed stability constants are already well resolved, the algorithm can stop.

# Acknowledgment

The authors would like to thank Prof. Karen Veroy (RWTH Aachen) for pointing out reference [4].

# References

[1] G. Rozza, D. B. P. Huynh, and A. T. Patera, "Reduced Basis Approximation and a Posteriori Error Estimation for Affinely Parametrized Elliptic Coercive Partial Differential Equations," *Archives of Computational Methods in Engineering*, vol. 15, pp. 229 – 275, 2008.

[2] M. W. Hess and P. Benner, "Fast Evaluations of Time-Harmonic Maxwell's Equations Using the Reduced Basis Method," *IEEE Transactions on Microwave Theory and Techniques*, vol. 61, pp. 2265 – 2274, 2013.

[3] ——, "Reduced Basis Modeling for Time-Harmonic Maxwell's Equations," *COMPEL - The international journal for computation and mathematics in electrical and electronic engineering*, vol. 33, no. 4, pp. 1071 – 1081, 2014.

[4] Y. Maday, A. T. Patera, and D. V. Rovas, "A Blackbox Reduced-Basis Output Bound Method for Noncoercive Linear Problems," *Studies in Mathematics and its Applications*, vol. 31, pp. 533 – 569, 2002.

[5] K. K. Stavrakakis, T. Wittig, W. Ackermann, and T. Weiland, "Linearization of Parametric FIT-Discretized Systems for Model Order Reduction," *IEEE Transactions on Magnetics*, vol. 45, pp. 1380 – 1383, 2009.

[6] D. Schmidthaeusler and M. Clemens, "Low-Order Electroquasistatic Field Simulations Based on Proper Orthogonal Decomposition," *IEEE Transactions on Magnetics*, vol. 48, pp. 567 – 570, 2012.

[7] B. H. N. Jung, A.T. Patera and B. Lohmann, "Model Order Reduction and Error Estimation with an Application to the Parameter-Dependent Eddy Current Equation," *Mathematical and Computer Modelling of Dynamical Systems*, vol. 17, pp. 561 – 582, 2011.

[8] R. Hiptmair, "Finite Elements in computational electromagnetism," *Acta Numerica*, pp. 237 – 339, 2002.

[9] Y. Chen, J. S. Hesthaven, Y. Maday, and J. Rodriguez, "Improved Successive Constraint Method Based A Posteriori Error Estimate for Reduced Basis Approximation of 2D Maxwell's Problem," *ESAIM: Mathematical Modelling and Numerical Analysis*, vol. 43, pp. 1099 – 1116, 2009.

[10] M. L. Stein, "Interpolation of Spatial Data. Some Theory for Kriging," *New York, NY: Springer*, 1999.

[11] V. Hernandez, J. E. Roman, and V. Vidal, "SLEPc: A scalable and flexible toolkit for the solution of eigenvalue problems," *ACM Transactions on Mathematical Software*, vol. 31, no. 3, pp. 351–362, 2005.

[12] E. Romero and J. E. Roman, "A parallel implementation of Davidson methods for large-scale eigenvalue problems in SLEPc," *ACM Transactions on Mathematical Software*, vol. 40, no. 2, pp. 13:1–13:29, 2014.

[13] ——, "Computing subdominant unstable modes of turbulent plasma with a parallel Jacobi-Davidson eigensolver," *Concurrency and Computation: Practice and Experience*, vol. 23, no. 17, pp. 2179–2191, 2011.

[14] M. S. Handcock, "On Cascading Latin Hypercube Designs and Additive Models for Experiments," *Communications in Statistics - Theory and Methods*, vol. 20, pp. 417 – 439, 1991.

[15] S. N. Lophaven, H. B. Nielsen, and J. Søndergaard, "DACE-A Matlab Kriging toolbox, version 2.0," Tech. Rep., 2002.

[16] D. Gorissen, K. Crombecq, I. Couckuyt, T. Dhaene, and P. Demeester, "A surrogate modeling and adaptive sampling toolbox for computer based design," *Journal of Machine Learning Research*, vol. 11, pp. 2051 – 2055, 2010.